UPPER TROPOSPHERIC DIVERGENCE FIELDS IN A TROPICAL CONVECTIVE SYSTEM OBSERVED WITH METEOSAT-8

Johannes Schmetz, Regis Borde, Marianne König and Hans-Joachim Lutz

EUMETSAT, D-64295 Darmstadt, Germany

ABSTRACT

The paper studies the diurnal variation of divergence of the upper level wind field in tropical deep convective systems as observed by Meteosat-8. The wind field divergence is computed in two ways: a) from atmospheric motion vectors (AMVs) derived by tracking of cloud and water vapour features in the water vapour channel at 6.2 μm, and b) from the relative change in time of the coverage with convectively active clouds. Both methods give consistent results with maximum divergence values larger than 30.10^{-5} s^{-1}. Taking the height of the AMVs as mean level of divergence the height of the divergence ranges from 200 to 150 hPa. The scale of the derived tropical upper tropospheric divergent fields is of the order of 300 – 500 km. The observed divergence fields are about an order magnitude lager than those in the corresponding ECMWF analysis. It is also suggested that the currently performed thinning of AMVs in NWP assimilation systems may alias incorrect spatial features of upper level divergence fields into the analysis. In view of this difficulty of NWP models to assimilate the high density AMVs it is proposed to consider a gridded product of upper tropospheric divergence for assimilation in NWP models.

1. INTRODUCTION

In tropical regions diurnal cycles of deep convective cloud systems are commonly observed. Those diurnal cycle are most pronounced over the continents and most often forced by the daily course of the solar surface heating. Typically the diurnal cycle of convective systems over land leads to minima of the OLR in the afternoon and early evening which is asscociated with a maximum in precipitation (e.g. Gray and Jacobson, 1977; Hendon and Woodberry, 1993). Previous satellite studies of the diurnal cycle mainly addressed clouds and were based on thermal IR window channel observations. This paper studies the direct inference of the diurnal cycle of upper tropospheric wind divergence in tropical convective systems from satellite imagery. The case study based on Meteosat-8 data, which is the first satellite of the second generation of Meteosats with twelve spectral channels (versus three for the 1st generation), a spatial sampling distance of 3 km (versus 5 km for the 1st generation) and a full disk imaging repeat cycle of 15 minutes (versus 30 minutes). A detailed introduction to Meteosat Second Generation is provided in Schmetz et al. (2002).

2. DATA

The area chosen for this study extends from 9.6°N – 15.6°S and 8.1°E – 36.7°E over central Africa corresponding to nearly 3000 km x 3000 km represented by more than 800000 pixels. Image data and products (i.e. Atmospheric Motion Vectors and Cloud Analysis) are from Meteosat-8 for 29 March 2004 from 0000 – 2400 UT. In addition to the satellite data, ECMWF temperature analysis data have been used as auxiliary data for cloud analysis. Figure 1 shows the area averaged profiles of potential (depicted by +) and equivalent potential temperature (*) for the study area from the ECMWF analysis; there the conditionally unstable air in the mid-troposphere is clearly depicted in the vertical profile of the equivalent potential temperature. The following subsections explain how the geophysical parameters are derived.

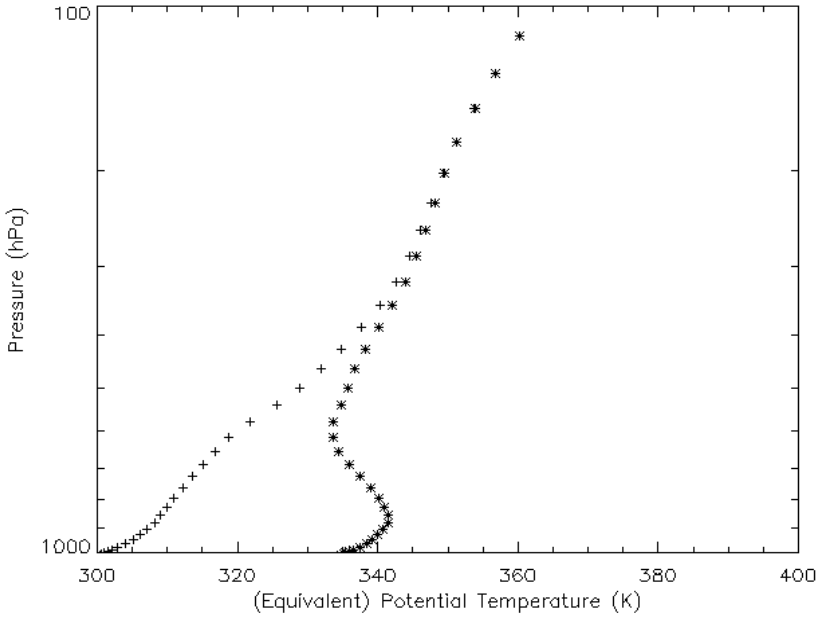

Figure 1: Area averaged profiles of potential and equivalent potential temperature from the ECMWF analysis.

2.1. Wind field and divergence

Atmospheric Motion Vectors (AMVs) have been derived from tracking cloud and humidity features in the 6.2 µm WV channel of Meteosat-8 using the Meteosat Second Generation (MSG) prototype algorithm (Holmlund, 2000a). The vectors are derived with a cross-correlation technique using a 24x24 pixel template and searching in a area of 20x20 pixels, implying a small overlap. The wind fields are quality controlled following Holmlund (1998) and vectors with are quality indicator (QI) higher than 0.5 are retained.

Earlier work has shown that it is difficult to infer divergence fields directly from the wind vectors since the differentiation amplified the noisy character of the wind field; e.g. Schmetz et al. (1995) used monthly averages of divergence fields in order to reduce the noise. In order to derive instantaneous divergence fields from the AMV field, a QI-weighted Barnes filter has been run over the wind vectors before computing the divergence with finite differences over areas of 3x3 pixels as described in Holmlund (2000b). The weights are computed from:

$$w = \exp\left[-\left(\frac{\Delta r}{r_o}\right)^2 - \left(\frac{\Delta t}{t_o}\right)^2 - \left(\frac{1-qi}{qi_o}\right)^2 \right] \quad (1)$$

with r_o = 2° lat/long; t_o = 0.5 h; qi_o = 0.4. Δt is set to zero here.

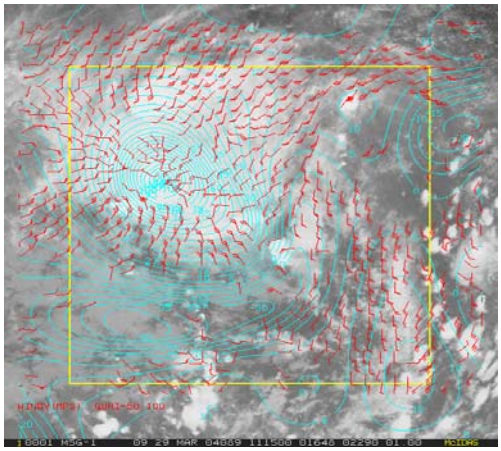

Figure 2: Study area depicted by the blue frame and derived atmospheric motion vectors (AMVs) for 1115 UT on 29 of March 2004. Isolines give the upper tropospheric divergence pattern derived from the AMVs derived by tracking in the 6.2 µm channel.

Figure 2 shows the study area, the derived atmospheric motion vectors (AMVs) and the divergence field obtained from the AMVs for 1115 UT on 29 March 2004. In the NW quadrant of the study area a large-scale convective system is observed which exhibits a distinct upper level divergence field. Several smaller scale convective cloud patterns can be discerned which later in the afternoon develop into larger deep convective cloud systems.

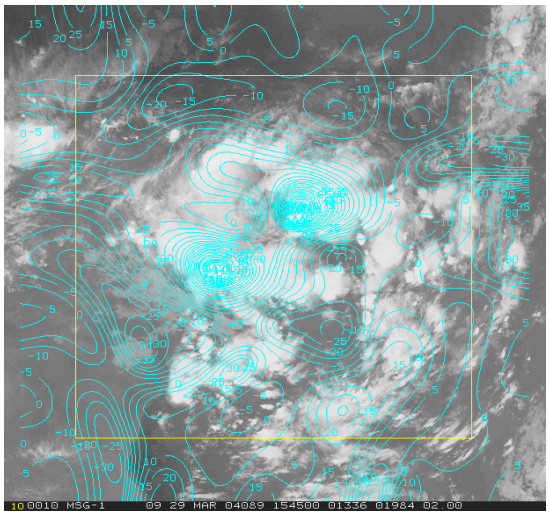

Figure 3: Upper tropospheric divergence fields at 1545 UT on 28 March 2004.

Figure 3 shows the divergence pattern inferred from atmospheric motion vectors (AMVs) at 1515h in the afternoon. Two divergence maxima are observed which coincide with clusters of developing deep convective clouds. Interesting is that the scale of the patterns is about 2° – 4° in latitude/longitude. This is a typical distance to which currently AMVs are thinned in global NWP assimilation (e.g. at ECMWF). Clearly such a thinned AMV field will not contain the real mesoscale structures of the wind field which are used to infer the divergence fields. In fact the thinning is likely to alias non-realistic structures into the analysis. 'Super-obing' (i.e. the averaging of individual AMVs) is also likely to delete the information on upper level mesoscale circulation. The analysis of high-density AMV products, as used in this study, does not seem to be possible either because of high spatial error correlation (Bormann et al., 2003). Therefore it appears consequential to propose the assimilation in NWP of a gridded divergence product which is directly inferred from high-level AMVs.

Figure 4 shows a time series of the divergence for the two cloud systems observed in Figure 3. While one system has an active phase of only five hours between about 1300h and 2000h, the second system is active from the early morning into the night. The absolute divergence maxima reach in both cases $4.5.10^{-4}$ s^{-1}. The divergence maxima have been obtained by tracking the migration of the convective systems manually, i.e. the advection of the systems has been taken out (Lagrangian approach).

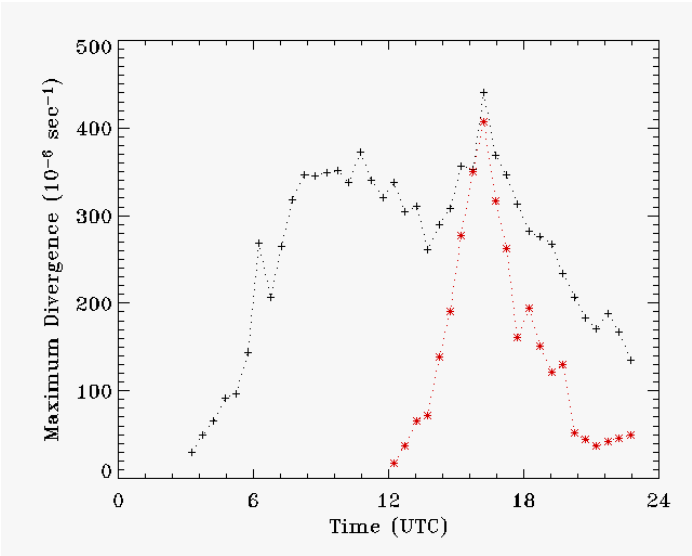

Figure 4: Diurnal cycle of the maximum of the upper tropospheric divergence fields for two convective systems on 28 March 2004.

An important question to be asked is, how large is the height variation of the divergence features in Figure 4 throughout the day? This is addressed in Figure 5 that gives the mean pressure height of the AMVs which are derived from successive images in the Meteosat-8 6.2 µm channel. The tracking includes cloud and water vapour structures. Figure 5 provides the mean pressure height and the standard deviation for the two divergence areas shown in Figure 4. The mean height has been computed from the AMVs (about 50 values) around the maximum of the divergence. In conclusion we see some variation in the mean height allocated to the divergence pattern which however is confined to about 50 hPa. Furthermore it is noted that tracking of clear sky water vapour and thin cloud tracers implies a tracking of a deep layer mean; as such the pressure heights depicted in Figure 5 have to be considered as 'representative height' and not as exact level of the inferred divergence.

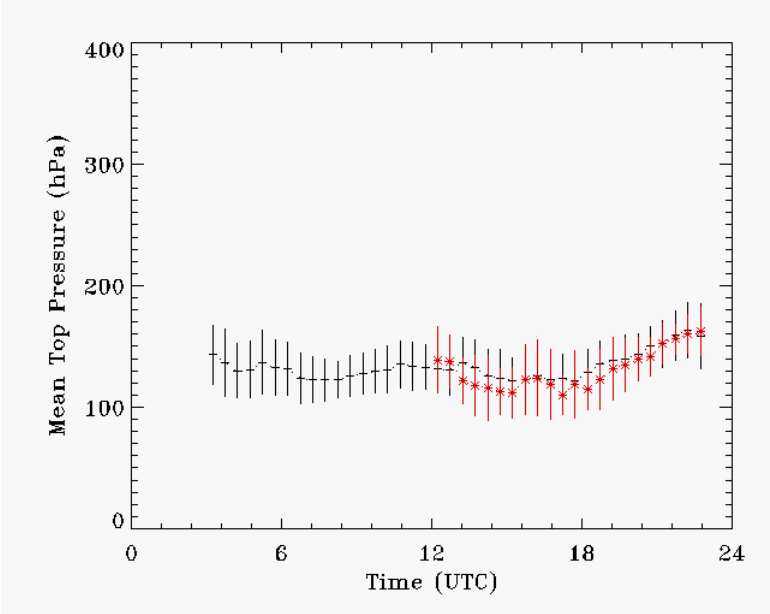

Figure 5: Height allocated to AMVs around the divergence maxima in Figure 4 and the standard deviation for the two fields of divergence.

2.2. Divergence from convectively active cloud

This section explores the possibility to derive a divergence field from the equation:

$$\nabla \cdot \vec{v} = \frac{dA}{A} \frac{1}{dt} \qquad (2)$$

where *A* is the cloud cover, *t* the time and v the wind vector. The approach follows Fraedrich et al. (1976) who estimated the upper level divergence from Equation 2 assuming that the relative rate of change in time of a horizontal area *A* of the cloud top outflow region is equal to the area-averaged horizontal wind divergence. In order to employ Equation 2 one needs to infer the cloud cover and its change from successive satellite images. Here we use the cloud cover information derived with the prototype algorithm developed for Meteosat Second Generation (Lutz, 1999). Figure 6 shows the diurnal variation of the number of high level convectively active clouds as defined by pixels where the brightness temperature in the 6.2 µm WV channel is higher than the brightness temperature at 10.8 µm (i.e. $T_{WV} > T_{IR}$). Schmetz et al. (1997) have suggested that cloud pixels fulfilling that criterion depict convectively active cloud elements, a concept that has been confirmed later by Soden (2000).

A further confirmation has been possible with Meteosat-8 data which indicate that cloudy areas with $T_{WV} > T_{IR}$ coincide well with areas containing small cloud particles which correspond to convective updraft regions (Rosenfeld, personal communication; Rosenfeld and Lensky, 1998). This relationship needs to be studied in more detail, however it suggests that the reason for $T_{WV} > T_{IR}$ is due to the cloud microphysics.

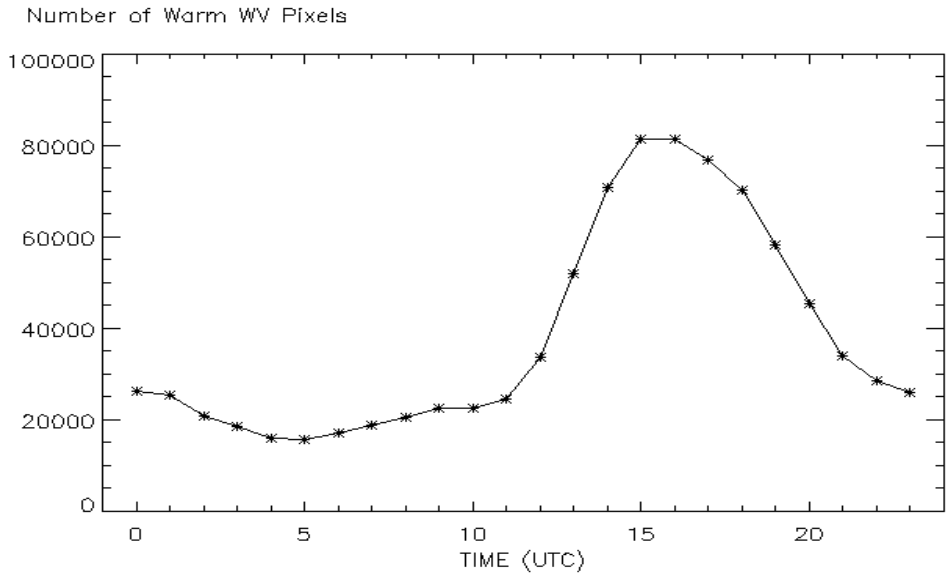

Figure 6: Diurnal cycle of the number of pixels in the study area (see Figure 2) with $T_{WV} > T_{IR;}$ i.e. with brightness temperature in the 6.2 µm water vapour channel exceeding the brightness temperature in the infrared window channel at 10.8.µm.

Using the relative change of the number of pixels with $T_{WV} > T_{IR}$ between 1100h and 1500h Equation 2 gives a value for the divergence of 2.9 10^{-4} s^{-1} which is in fairly good agreement with the maximum divergence values derived from the AMVs.

It should be noted that the use of the total high level cloud cover provides inconsistent results which are about an order of magnitude lower. This is due to the fact that a large fraction of high cloud cover consists of inactive decaying cloud, which compensates largely for the changes in active cloud.

Temperature threshold	<220 K	<210 K	<200 K	<195 K	<190 K
Divergence in 10^{-4} s^{-1}	1.2	1.5	2.1	3.	4.3

Table 1: Upper level divergence in 10^{-4} s^{-1} derived from Equation 2 using the pixels with brightness temperatures colder than the threshold in the 10.8µm channel.

Another way of defining active clouds is through brightness temperature thresholds in the channel at 10.8 µm. This has been done in Figure 7 which shows the diurnal cycle of the fractional cloud cover with temperatures colder than a given threshold (here: < 220 K, <210 K, < 200 K, < 195 K and < 190 K). Table 1 shows the divergence values derived from the relative changes in fractional cloud cover with pixels colder than the threshold. As expected the divergence values increase with decreasing temperature threshold. For low temperature (190 and 195 K), which are indicative of convectively active clouds, we find again reasonable agreement with values derived from AMVs.

3. COMPARISON WITH ECMWF

Figure 8 shows a comparison of divergence fields in the ECMWF analysis (right panel) with the corresponding observation from Meteosat-8 (left panel) on 29 March 2004 at 1200 UT. Is easily observed that there is little similarity, neither in structure nor in magnitude; in fact ECMWF analysis values are about an order of magnitude smaller. This observation requires further study and may (or not) corroborate the proposal to develop a gridded divergence product for assimilation in NWP.

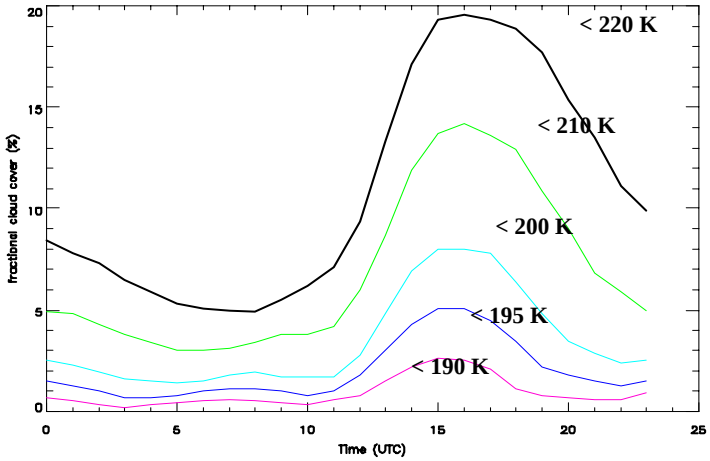

Figure 7: Diurnal cycle of the fractional coverage with pixels with T_{IR} lower than a given threshold. The temperature thresholds are indicated in the figure.

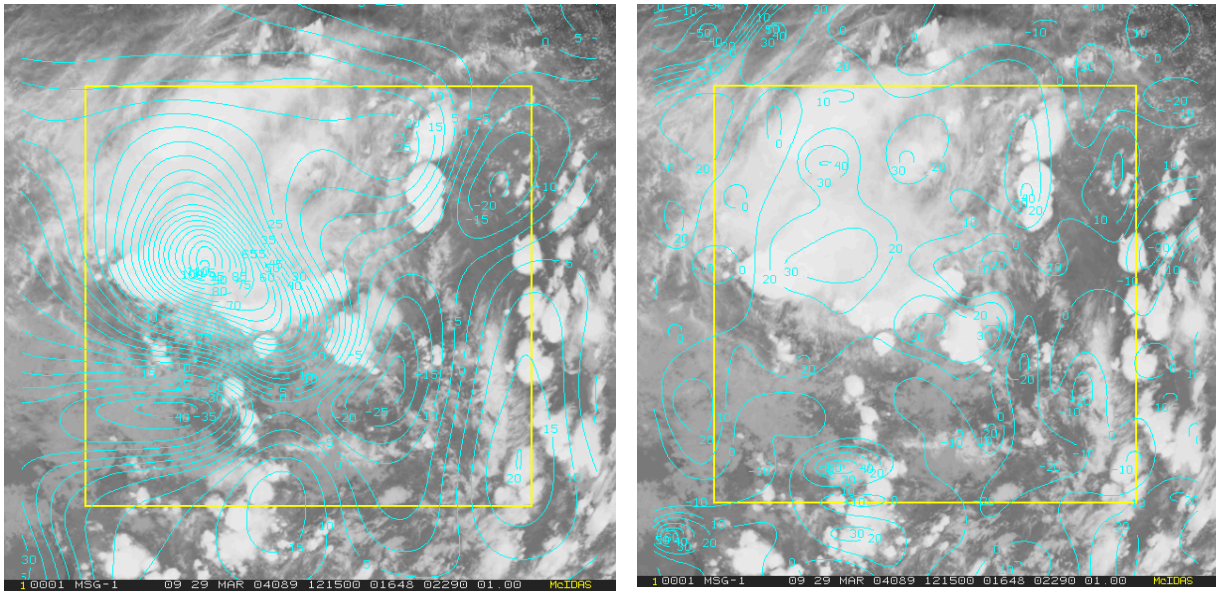

Figure 8: Left panel divergence field derived from AMVs at 1215 UT; right panel corresponding divergence field at 150 hPa in the ECMWF analysis at 1200 UT.

4. CONCLUSIONS

The main conclusions can be summarised as follows:

- The upper tropospheric wind field divergence in tropical deep convective systems can be estimated directly from atmospheric motion vectors inferred from WV channel observations at 6.2 μm of Meteosat-8. The diurnal cycle of divergence reaches maxima larger than $30 \cdot 10^{-5}$ s^{-1}.
- The derived tropical divergence fields have a scale of about 300 - 500km
- The variation of the 'mean' altitude of the observed divergence field, as defined by the mean height of AMVs near the location of the maximum of divergence, varies only by about 50 hPa throughout the day.
- The upper tropospheric wind field divergence in tropical deep convective systems can also be inferred from the relative change of high level convectively active clouds. Divergence values are consistent with those derived from AMVs. Convectively active cloud have been defined by pixels with brightness temperatures $T_{WV} > T_{IR}$ or with T_{IR} colder than a threshold (190 K or 195 K). This suggests an even simpler way of deriving an upper level divergence product.

- Thinning and/or superobbing of AMVs at a scale of several 100 km as currently performed in NWP data assimilation potentially damages the analysis because 'non-real' information could be is aliased into the analysis field.
- It is suggested to develop a gridded divergence product for NWP which would circumvent the problems associated with the high spatial error correlation of AMVs which currently necessitates the thinning.

5. REFERENCES

Bormann, N., S. Saarinen, G. Kelly and J.N. Thepaut, 2003: The spatial structure of observation errors in atmospheric motion vectors from geostationary saetllite data. *Mon. Wea. Rev*. 131, 706 – 718.

Fraedrich, K., E. Ruprecht and U. Trunte, 1976: Determination of the cirrus outflow divergence as seen by satellite. *J. Appl. Meteorol.*, 15, 1312 – 1316, 1976.

Gray, W.M. and R.W. Jacobson, 1977: Diurnal variation of deep cumulus convection. *Mon. Wea. Rev*., 105, 1171-1188.

Hendon, H.H. and K. Woodberry, 1993: The diurnal cycle of tropical convection. *J. Geophys. Res*., 98, D9, 16623 – 16637.

Holmlund, K., 1998: The utilization of statistical properties of satellite-derived atmospheric motion vectors to derive quality indicators. *Wea. Forecasting*, 13, 1093 – 1104.

Holmlund, K., 2000a: The Atmospheric Motion Vector retrieval scheme for Meteosat Second Generation. Proc. Fifth Int. Winds Workshop, Lorne, Australia, EUMETSAT, EUM-P28, 201-208.

Holmlund, K., 2000b: The use of Observations error as an extension to Barnes interpolation scheme to derive smooth instantaneous vector fields from satellite-derived Atmospheric Motion Vectors. Proceedings of the 5th International Winds Workshop, Lorne, Australia.

Lutz, H.J., 1999: Cloud processing for Meteosat Second Generation. EUMETSAT Tech. Department Tech. Memo. 4, 26pp.

Peixoto, J.P. and A.H. Oort, 1992: Physics of climate, American Institute of Physics, pp. 520.

Rosenfeld, D. and I. M. Lensky, 1998: Satellite-based insights into precipitation formation processes in continental and maritime convective clouds. *Bull. Amer. Meteor. Soc*., 79, 2457 – 2476.

Schmetz, J., C. Geijo, W.P. Menzel, K. Strabala, L. van de Berg, K. Holmlund and S. Tjemkes, 1995: Satellite observations of upper tropospheric relative humidity, clouds and wind field divergence. *Contrib. Atmosph. Physics*, 68, 345 - 357.

Schmetz, J., S.A. Tjemkes, M. Gube and L. van de Berg, 1997: Monitoring deep convection and convective overshooting with Meteosat. *Adv. Space Res*., Vol. 9, No. 3, 433-441.

Schmetz, J., P. Pili, S. Tjemkes, D. Just, J. Kerkmann, S. Rota and A. Ratier, 2002: An Introduction to Meteosat Second Generation (MSG). *Bull. Amer. Meteor. Soc*., 83, 977 – 992.

Soden, B.J., 2000: The diurnal cycle of convection, clouds, and water vapor in the tropical upper troposphere. *Geophys. Res. Letters*, 27, 2173-2176.